Analysis of the Geomagnetic Activity of the *Dst* Index and Self-Affine Fractals Using Wavelet Transforms

H.L. Wei , S.A. Billings and M. Balikhin

RERVM COGNOSCERE CAVSAS

Research Report No. 846

Department of Automatic Control and Systems Engineering
The University of Sheffield
Mappin Street, Sheffield,
S1 3JD, UK

Oct. 2003

Analysis of the Geomagnetic Activity of the *Dst* Index and Self-Affine Fractals Using Wavelet Transforms

H.L. Wei , S.A. Billings and M. Balikhin *

Department of Automatic Control and Systems Engineering, University of Sheffield
Mappin Street, Sheffield, S1 3JD, UK

The geomagnetic activity of the *Dst* index is analyzed using wavelet transforms and it is shown that the *Dst* index possesses properties associated with self-affine fractals. For example, the power spectral density obeys a power-law dependence on frequency, and therefore *Dst* can be viewed as a self-affine fractal dynamic process. It is shown that the wavelet covariance exponent, which is based on wavelet variance analysis, is identical to the power-law exponent for a time series with a power spectral density which obeys a power-law dependence on frequency. Therefore the wavelet covariance exponent provides a direct measure of the strength of persistence of the *Dst* indices. One of the advantages of wavelet analysis is that many inherent problems encountered in Fourier transform methods, such as windowing and detrending, are not necessary.

Keywords: wavelet transform; fractals; self-affine; geomagnetic activity; power-law

1. Introduction

The magnetosphere can be considered as a complex input-output system. For such a system, the solar wind plays the role of the input and the geomagnetic indexes can be considered as outputs. Properties of the output data sets can be used to analyse and to understand properties of the dynamical system itself. In the present paper, properties of the *Dst* index are studied to aid the understanding of properties of the complex magnetospheric dynamical system.

Several approaches have been proposed to analyse the *Dst* and other geomagnetic activity indices. These include autonomous data analysis, analogue modelling, and input-output observational data-based modelling approaches, see for example, the review by Klimas et al. (1996). Auto-correlation and spectral analysis, phase-space reconstruction and invariant property analysis of chaotic behaviours in these indices are often based on autonomous data analysis (Baker et al. 1990, Vassiliadis 1990, Shan et al 1991, Roberts et al 1991, Takalo et al. 1993, Takalo and Timonen 1994a, 1994b, Zotov 2000). The analogue modelling approach which aims to build low-dimensional dynamic analogue systems that can be used to interpret the physical interactions in the magnetosphere and to forecast the geomagnetic indices, has been successfully applied by Goertz et al. (1993) and Klimas et al. (1997,1998,1999). Existing input-output observational data-based modelling approaches which haven been applied to these indices include ARMA models (see McPherron 1999, Vassiliadis 2000 and the references therein), neural networks (Hernandez et al 1993, Wu and Lundsted 1997), and NARMAX models (Boaghe et al 2001).

In this study the fractal invariance of the *Dst* index is analyzed using wavelet transforms. It is shown that the *Dst* index possesses properties of self-affine fractals, for example, the power spectral density obeys a power-law

(*) Corresponding author, email: balikhin@acse.shef.ac.uk

dependence on frequency, and therefore the *Dst* index can be viewed as a self-affine fractal dynamic process. Fractal invariance studies alone do not generally reveal the underlying physics. However, the fractal structure of the *Dst* index does add to the information needed to find the physical mechanism responsible for this phenomenon. The fractal dimension estimated from the power exponent also provides information regarding the choice of an appropriate embedding dimension for the dynamic modelling and forecasting of this index.

2. The *Dst* index as a self-affine dynamic process

The term fractal, introduced by Mandelbrot (1983), involves three related contexts: geometric, temporal (dynamic) and statistical fractals. Generally, the concept of a fractal is defined in terms of self-similarity. A great number of natural phenomena in physics, geometry, ecology, physiology and topography have been shown to exhibit self-similarity (Goldberger 1992, Turcotte 1997, Li 2000, Sahimi 2000, Xiong et al 2001).

2.1 Self-affine fractals

A self-affine set is statistically invariant under an affine transformation. An n-dimensional super-surface described by a function $f(x_1, x_2, \cdots, x_n)$ is a self-affine fractal, if there exists a number H such that

$$f(x_1, x_2, \cdots, x_n) = C(\lambda_1^H, \lambda_2^H, \cdots, \lambda_n^H) f(\lambda_1 x_1, \lambda_2 x_2, \cdots, \lambda_n x_n) \tag{1}$$

where $C(\lambda_1^H, \lambda_2^H, \cdots, \lambda_n^H)$ is a deterministic function of λ_i^H, and $\lambda_i (i = 1,2,\cdots,n)$ are positive numbers. H is called the Hurst exponent or Hausdorff exponent or self-affine exponent, with a value generally falling into the interval [0,1]. In one-dimensions, a self-affine fractal (Mandelbrot 1983, Turcotte 1997) is defined as $f(x) = \lambda^{-H} f(\lambda x)$. In this case, x and $f(x)$ are often interpreted as the time and the corresponding trajectory (position), respectively. Voss (1988) proved that the Hurst exponent, H, and the self-affine fractal dimension, or the box-counting dimension, D, are related by the equation H=2-D. Therefore $1 \le D \le 2$ corresponds to $0 \le H \le 1$ for a self-affine fractal. If H=1, the self-affine fractal becomes self-similar.

Following Turcotte (1997) and Turcotte and Malamud (1999), the basic definition of a self-affine time series is that the power spectral density of the time series has a power-law dependence on frequency.

2.2 Spectral analysis for the *Dst* index

The physical features of a dynamic system can be easily detected and revealed using frequency domain analysis, which is often implemented by means of Fourier transforms of the covariance functions. The main point of this section is to show that the power spectral density of the *Dst* indices obeys a power-law dependence on frequency

$$P(\omega) \propto |\omega|^{-\beta} \tag{2}$$

As an example, the *Dst* indices for the years from 1981 to 2000 were considered and the power spectra for the *Dst* indices of each year were calculated separately and are shown in Figure 1, where the sampling period for each yearly index is 1 hour and the frequency has been normalised. The average of the 20 power spectral density functions is plotted in Figure 2(the solid line). The *Dst* indices over the 20 years can also be considered as a single signal $s(t)$ consisting of 175800 points. The power spectrum of this signal was estimated and is also shown in Figure 2, where again the frequency has been normalised. Figures 1 and 2 clearly show that the power spectra of the *Dst* indices obey a power-law in the sense that $P(f) \propto |f|^{-\beta}$, where $\beta \approx 2$. This suggests that the *Dst* indices can be considered as a self-affine time series and the power exponent $\beta>1$ here indicates that the process of the *Dst* indices is strongly persistent. The broadband spectra of the *Dst* indices also indicates that a potential chaotic behaviour may exist in the dynamic process.

3. Analysis of the *Dst* index using wavelet transforms and wavelet decompositions

Just as Fourier series can be used to superimpose sines and cosines to represent other functions, wavelets are functions that possess certain properties that can be used to represent complex signals. However, wavelets differ greatly from Fourier series. Unlike the Fourier basis functions, wavelet basis functions have the property of localisation both in time and frequency. Due to this inherent property, wavelet approximation provides the foundation for representing arbitrary signals economically, using just a small number of wavelets. In wavelet analysis, the scale that is used to analyse the data plays a special role.

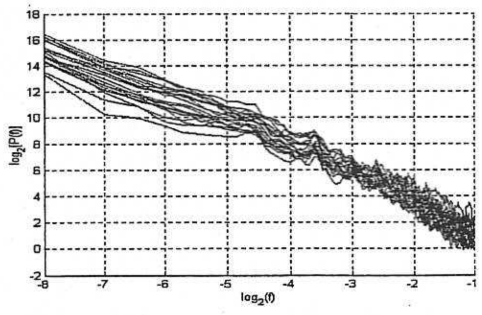

Fig. 1 The power spectra of the *Dst* indices for the years from 1981 to 2000 with a sampling period of 1 hour for each yearly index. The slope of the spectral lines is approximately 2.

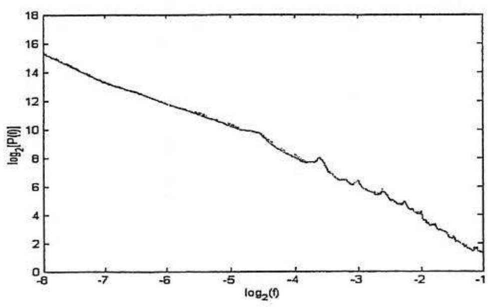

Fig. 2 The average of the power spectral density functions of the D_{st} indices for the years from 1981 to 2000(the solid line) and the overall power spectral density function of the Dst indices of 20 years (the dashed line). The average slope of the spectral line is approximately 2.

The wavelet analysis procedure consists of adopting a wavelet prototype function, called the *analysing wavelet* or *mother wavelet* or simply *wavelet.* Temporal analysis is performed with a contracted, high-frequency version of the same function. Because the signal to be analysed can be represented in terms of a wavelet expansion, data operations can be performed using only the corresponding wavelet coefficients.

Wavelets have an excellent approximation capability, that is why wavelet theory has so many applications in many diverse fields, namely signal and image processing, speech analysis, fault detection, fractals, system identification and so on. The wavelet transform also possesses a property of self-similarity. This makes wavelets particularly useful for dealing with nonperiodic and nonstationary multiscaled time series, including signals with self-similarity (Wornell 1996) and fractional Brownian motion (Malanmud and Turcotte 1999).

3.1 Wavelet transforms

Let f be a function defined in $L^2(R)$. The continuous wavelet transform (CWT) with respect to the *mother wavelet* ψ is defined as (Chui 1992, Daubechies 1992).

$$W_f^{\psi}(b,a)=\frac{1}{\sqrt{a}}\int_{-\infty}^{+\infty} f(t)\overline{\psi\left(\frac{t-b}{a}\right)}dt \tag{3}$$

with the dilation (scale) parameter $a \in R^+$ and the shift (translation) parameter $b \in R$. The over-bar above the function $\psi(\cdot)$ indicates complex conjugate. The continuous wavelet transform (3) is invertable subject to a mild restriction imposed on the wavelet φ, in the sense that

$$f(t)=\frac{1}{C_{\psi}}\int_{-\infty}^{\infty}\frac{da}{a^2}\int_{-\infty}^{\infty}[W_f^{\psi}(b,a)]\frac{1}{\sqrt{a}}\psi\left(\frac{t-b}{a}\right)db \tag{4}$$

with

$$C_{\psi}=\int_{-\infty}^{\infty}\frac{|\hat{\psi}(\omega)|^2}{|\omega|}d\omega<\infty \tag{5}$$

where $\hat{\psi}(\cdot)$ is the Fourier transform of the function $\psi(\cdot)$. The inverse transform (4) guarantees that the function $f(x)$ can be reconstructed from the CWT and it can be interpreted in at least two different ways. On the one hand, this shows how to reconstruct the function f from the wavelet transform and, on the other hand, the inverse transform gives a recipe showing how to write any arbitrary f as a superposition of wavelet functions $\psi((t-b)/a)$.

It is easy to verify that the continuous wavelet transform (3) possesses the following basic properties:

(i) Shift property. Let $f \in L^2(R)$ *and* $g(t)=f(t-t_0)$, $t_0 \in R$, *then*

$$W_g^{\psi}(b,a)=W_f^{\psi}(b-t_0,a) \tag{6}$$

(ii) Scale property. Let $f \in L^2(R)$ *and* $g(t)=f(\lambda t)$, $\lambda>0$, *then*

$$W_g^{\psi}(b,a)=\frac{1}{\sqrt{\lambda}}W_f^{\psi}(\lambda b,\lambda a) \tag{7}$$

(iii) Self-similarity property. Let $f \in L^2(R)$, *satisfying* $f(\lambda t)=\lambda^H f(t)$ *for similarity parameter* $H>0$ *and any real number* $\lambda>0$ *, then*

$$W_f^{\psi}(b,a)=\lambda^{-(H+\frac{1}{2})}W_f^{\psi}(\lambda b,\lambda a) \tag{8}$$

Figure 3 is a 3-D plot showing the wavelet transform (3) of the *Dst* index from 1st July to 30th September, 2000, consisting of 2202 data points with a sampling interval of 1 hour, where the second order Daubechies wavelet (Daub2) was adopted. It can be seen from the Figure 3 that the wavelet amplitude $\left|W_f^{\psi}(b,a)\right|$ becomes stronger when the frequency becomes lower (which corresponds to a large scale factor *a*). This is an important property of a self-affine process (Malamud and Turcotte 1999) with the power exponent $\beta > 1$. The image of the wavelet coefficients for the scale level $1 \leq a \leq 128$ is shown in Figure 4.

3.2 Wavelet decompositions

Under some assumptions and considerations, an orthogonal wavelet system can be constructed using *multiresolution analysis* (MRA)(Mallat 1989, Chui 1992). Assume that the wavelet ψ and associated scaling function ϕ constitute an orthogonal wavelet system, then any function $f \in L^2(R)$ can be expressed as a *multiresolution wavelet decomposition*

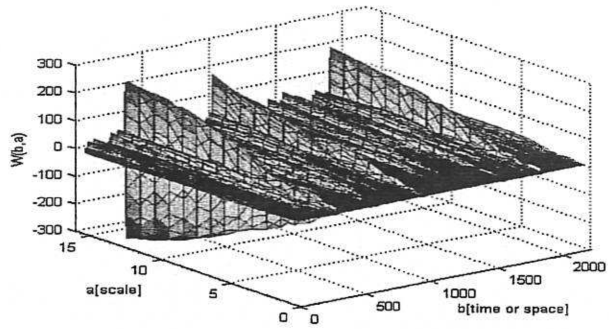

Fig. 3 The continuous wavelet transform of the Dst index from 1st July to 30th September, 2000, consisting of 2202 data points with a sampling interval of 1 hour. The 2nd order Daubechies wavelet (Daub2) was used and the range for the scale parameter a is $0.5 \leq a \leq 16$.

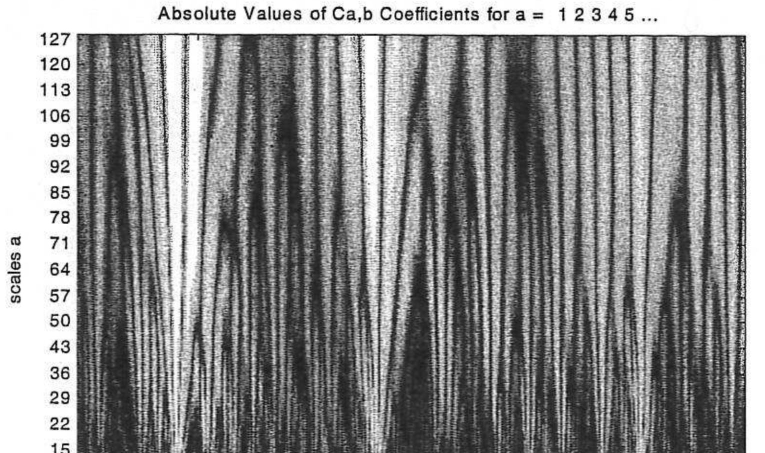

Fig. 4 The image of the wavelet transform of the Dst index from 1st July to 30th September, 2000, consisting of 2202 data points with a sampling interval of 1 hour. The 2nd order Daubechies wavelet (Daub2) was used and the range for the scale parameter a is $1 \leq a \leq 128$.

$$f(x) = \sum_k a_{j_0,k}\phi_{j_0,k}(x) + \sum_{j\geq j_0}\sum_k d_{j,k}\psi_{j,k}(x) \tag{9}$$

where $\psi_{j,k}(x) = 2^{j/2}\varphi(2^j x - k)$ and $\phi_{j,k}(x) = 2^{j/2}\phi(2^j x - k)$, $j,k \in Z$, and the wavelet approximation coefficient $a_{j_0,k}$ and the wavelet detail coefficient $d_{j,k}$ can be calculated in theory by the inner products:

$$a_{j_0,k} = < f, \phi_{j_0,k} > = \int f(x)\overline{\phi_{j_0,k}(x)}dx \tag{10}$$

$$d_{j,k} = < f, \psi_{j,k} > = \int f(x)\overline{\psi_{j,k}(x)}dx \tag{11}$$

and j_0 is an arbitrary integer representing the lowest resolution or scaling level.

The *Dst* index of the year 2000 consisting of 8808 data points with a sampling interval of 1 hour was decomposed into the multiresolution wavelet decomposition (9), where the second order Daubechies wavelet (Daub2) was used. The wavelet approximation coefficients $a_{j,k}$ and the detail coefficients $d_{j,k}$ are shown in Figures 5 and 6. Again, it can be clearly seen from Figures 5 and 6 that the amplitudes of the wavelet coefficients become stronger when the frequency becomes lower (which corresponds to a large minus *j*). This is an important property of a self-affine process with the power exponent $\beta > 1$.

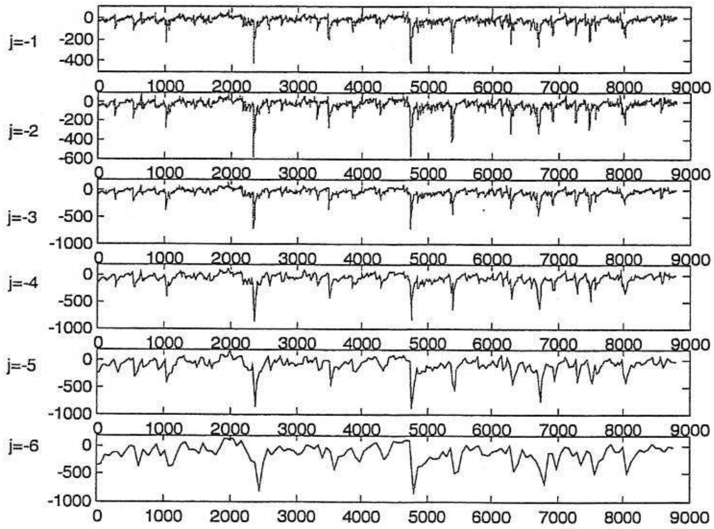

Fig. 5 The wavelet approximations at scale 2^j computed with Daub2 for the Dst index of the year 2000, consisting of 8808 data points with a sampling interval of 1 hour.

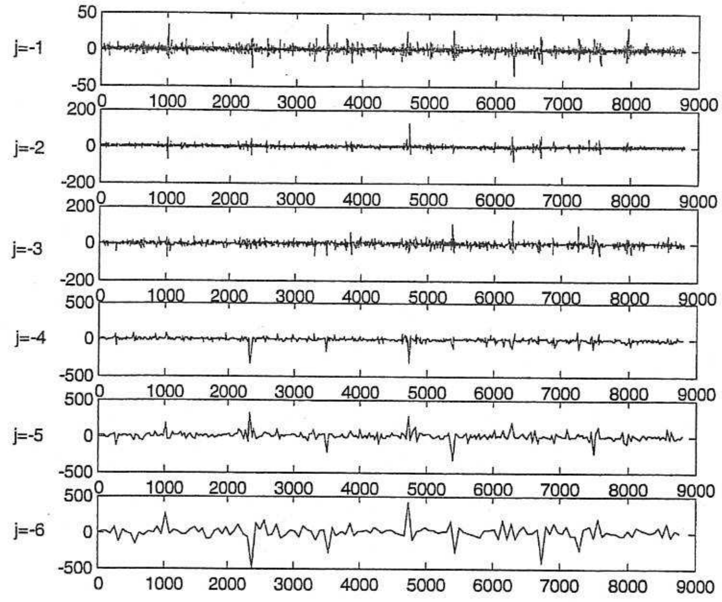

Fig. 6 The wavelet details at scale 2^j computed with Daub2 for the Dst index of the year 2000, consisting of 8808 data points with a sampling interval of 1 hour.

3.3 Wavelet transform covariance

Following Flandrin (1989), the covariance of the wavelet transform (3) of a signal $x(t)$ at a given scale a can be defined as

$$R_x^{\psi}(t,s;a) = E[W_x^{\psi}(t,a)\overline{W_x^{\psi}(s,a)}] \tag{12}$$

It can be shown by means of the convolution theory and Parseval's identity that

$$R_x^{\psi}(t,s;a) = \frac{a}{2\pi}\int_{-\infty}^{\infty} P_x(\omega)\left|\hat{\psi}(a\omega)\right|^2 e^{-i(t-s)\omega}\,d\omega \tag{13}$$

where $P_x(\omega)$ is the power spectrum of the signal $x(t)$. If $x(t)$ is a self-affine signal obeying the power-law (2) with a power exponent β then the auto-covariance of the wavelet transform also obeys a power-law in the sense that

$$R_x^{\psi}(t;a) = E[W_x^{\psi}(t,a)\overline{W_x^{\psi}(t,a)}] = \frac{a}{2\pi}\int_{-\infty}^{\infty}\frac{\left|\hat{\psi}(a\omega)\right|^2}{\left|\omega\right|^{\beta}}d\omega = \frac{a^{\beta}}{2\pi}\int_{-\infty}^{\infty}\frac{\left|\hat{\psi}(\omega)\right|^2}{\left|\omega\right|^{\beta}}d\omega = Ca^{\beta} \tag{14}$$

where $C = \frac{1}{2\pi}\int_{-\infty}^{\infty}\frac{\left|\hat{\psi}(\omega)\right|}{\left|\omega\right|^{\beta}}$. Eq (14) suggests that for a self-affine signal $x(t)$, the covariance of the wavelet transform of signal $x(t)$ also obeys the power-law with a positive power β. The property of the wavelet transform covariance of Brownian motion has been studied in detail by Malamud and Turcotte (1999).

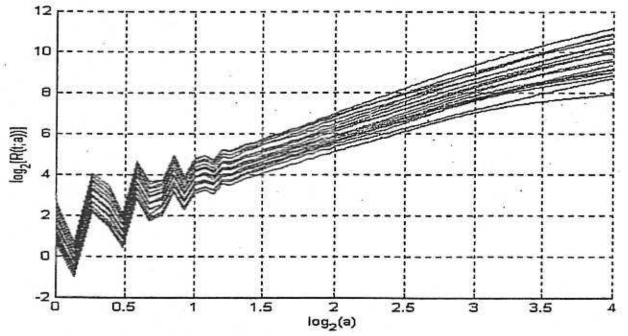

Fig. 7 The auto-variance of the wavelet transform of the Dst indices for the years from 1981 to 2000, the sampling period for the Dst indices of each year is 1 hour. The slope of the auto-covariance is approximately $\gamma \approx 2$.

Figure 7 shows the auto-covariance of the wavelet transform of the *Dst* indices for the years from 1981 to 2000. The slope of the auto-covariance function with respect to the scale factor $\log_2 a$ is about 2, which is identical with the power exponent estimated from the power spectral density where the value of the slope is approximately -2. This indicates that the auto-covariance function of the wavelet transform of the *Dst* indices obeys a power-law in the sense that $R^{\psi}_{Dst}(t;a) \propto |a|^{\gamma}$ with $\gamma \approx 2$.

4. Conclusions and discussions

The broadband and power-law dependence of the spectrum of the *Dst* index, identified in this study, clearly show that the *Dst* index possesses properties associated with self-affine fractals. The wavelet transform behaves like a microscope and decomposes a signal into amplitudes depending on dilations (scale) and translation (position). Multi-resolution decomposition enables a signal to be "observed" at higher and higher resolutions at different locations. These features of the wavelet transform along with the property of self-similarity, make wavelets particularly useful for dealing with nonperiodic and nonstationary multiscaled time series, including signals associated with self-affine and self-similar fractals. The power exponent of the *Dst* index obtained from the wavelet transform covariance is the same as that estimated from the traditional power spectral density. This means that, both the wavelet covariance method and the Fourier transform based power spectral approach give almost the same results for a long data set. However, numerous experiments show that for a short-time signal the wavelet covariance outperforms the Fourier transform based approach. Understanding the mechanisms of the self-affine fractal of the *Dst* index is helpful for building either an analogue model or an observational input-output data based model. Wavelet-based input-output nonlinear models can also be estimated and used to predict the *Dst* index (Wei et al 2002, Billings and Wei 2003).

Acknowledgment

The authors gratefully acknowledge that part of this work was supported by EPSRC.

References

Baker, D.N., Klimas, A.J., McPherron, R.L., and Buchner, J.(1990), The evolution from weak to strong geomagnetic activity: an interpretation in terms of deterministic chaos, *Geophysics Research Letter*, **17(1)**, 41-44.

Billings, S.A.and Wei, H.L.(2003), The wavelet-NARMAX representation: a hybrid model structure combining the polynomial models and multiresolution wavelet decompositions. (Submitted for publication).

Boaghe, O.M., Balikhin, M.A., Billings, S.A., and Alleyne, H.(2001), Identification of nonlinear processes in the magnetosphere dynamics and forecasting of *Dst* index, *Journal of Geophysical Research-Space Physics*, **106(A12)**, 30047-30066.

Chui, C. K.(1992), *An introduction to wavelets.* Boston : Academic Press.

Daubechies,I.(1992), *Ten lectures on wavelets*, Society for Industrial and Applied Mathematics, Philaelphia, Pennsylvania.

Flandrin, P.(1989), On the spectrum of fractional Brownian motions, *IEEE Transaction on Information Theory*, **35(1)**, 197-199.

Goertz, C.K., Shan, L.H., and Smith,R.A.(1993), Prediction of geomagnetic activity, *Journal of Geophysics Research-Space Physics*, **98(A5)**, 7673-7684.

Goldberger, A.L.(1992), Fractal mechanisms in the electrophysiology of heart, *IEEE Engineering in Medicine and Biology Magzine*, **11(2)**,47-52.

Hernandez, J.V., Tajima, T., and Horton, W.(1993), Neural net forecasting for geomagnetic activity, *Geophysical Research Letters*, **20(23)**, 2707-2710.

Klimas, A.J., Vassiliadis, D., Baker, D.N., and Roberts D.A.(1996), The organized nonlinear dynamics of the magnetosphere, *Journal of Geophysical Research-Space Physics*, **101(A6)**, 13089-13113.

Klimas, A.J., Vassiliadis, D., Baker, D.N.(1997), Data-derived analogues of the magnetospheric dynamics, *Journal of Geophysical Research-Space Physics*, **102(A12)**, 26993-27009.

Klimas, A.J., Vassiliadis, D., Baker, D.N.(1998),Dst index prediction using data-derived analogues of the magnetospheric dynamics, *Journal of Geophysical Research-Space Physics*,**103 (A9)**, 20435-20447.

Klimas, A.J., Vassiliadis, D., Baker, D.N., and Valdivia J.A.(1999), Data-derived analogues of the solar wind magnetosphere interaction, , *Phys. Chem.Earth (C)*, **24(1-3)**, 37-44.

Li, B.L. (2000), Fractal geometry applications in description and ananlysis of patch patters and patch dynamics, *Ecological Modelling*, **132(1-2)**, 33-50.

Malamud, B.D., and Turcotte, D.L.(1999), Self-affine time series: measures of weak and strong persistence, *Journal of Statistical Planning and Inference*, **80(1-2)**, 173-196.

Mallat,S.G.(1989),A theory for multiresolution signal decomposition: the wavelet representation, *IEEE Trans. On Pattern analysis and machine intelligence*, **11(7)**,674-693.

Mandelbrot, B.B.(1983), *The Fractal Geometry of Nature.* San Francisco, New York: W.H.Freeman and Company.

McPherron, R.L. (1999), Predicting the Ap index from past behaviour and solar wind velocity, *Phys. Chem. Earth (C)*, **24(1-3)**, 45-56.

Roberts,D.A., Baker,D.N, and Climas, A.J.(1991), Indications of low-dimensionality in magnetosphere dynamics, *Geophysical Research Letters*, **18(2)**, 151-154.

Shan, L.H., Hansen, P.,Goertz, C.K., and Smith, R.A.(1991), Chaotic appearance of the AE index, *Geophysical Research Letters*, **18(2)**, 147-150.

Sahimi,M.(2000), Fractal-wavelet neural-network approach to characterization and upscaling of fractal reservoirs, *Computers & Geosciences*, **26(8)**, 877-905.

Takalo, J., Timonen, J., and Koskinen, H.(1993), Correlation dimension and affinity of AE data and bicolored noise, *Geophysical Research Letters*, **20(15)**, 1527-1530.

Takalo, J., Timonen, J.(1994a), Characteristic time-scale of auroral electonjet data, *Geophysical Research Letters*, **21(7)**, 617-620.

Takalo, J., Timonen, J.(1994b), Properties of AE data and bicolored noise, *Journal of Geographical Reserch*, **99**, 13239-13249.

Turcotte, D.L.(1997), Fractals and Chaos in Geology and Geohysics (2nd ed), Cambridge: Cambridge University Press.

Wei, H.L., Billings, S.A., and Balikhin, M.A.(2003), Wavelet-based nonparametric models for nonlinear input-output system identification. (Submitted for publication).

Wornell, G.W.(1996), *Signal processing with fractals : a wavelet-based approach*, N.J. : Prentice Hall PTR; London : Prentice-Hall Inter.

Wu, J.G., and Lundsted, H.(1997), Neural network modelling of solar wind magnetosphere interaction, *Journal of Geophysics Research-Space Physics*, **102(A7)**,14457-14466.

Vassiliadis, D., Sharma, A.S., Eastman, T.E., and Papadopulos, K. (1990), Low-dimensional chaos in magnetospheric activity from AE time series, *Geophysical Research Letters*, **17(11)**, 1841-1844.

Vassiliadis, D., Klimas, A.J., Valdivia, J.A., and Baker, D.N., K. (2000), The nonlinear dynamics of space weather, *Phys. Chem. Earth (C)*, **26(1)**, 197-207.

Voss, R.F.(1988), *Fractals in nature : from characterization to simulation.* In *The Sceince of Fractal Images* edited by H.O. Peitgen and D. Saupe, New York: Springer.

Xiong, F., Jiang, X.Q., Gao, Y.S., and Li Z.(2001), Evaluation of engineering surface using a combined fractal modelling and wavelet analysis method, *International Journal of Machine Tools & Manufacture*, **41(13-14)**,2187-2193.

Zotov, O.D.(2000), Self-affine fractal dynamics of solar and earth magnetospheric activities, *Geomagnetism and Aeronomy*, **40(4)**, 439-443.